Research Article | Vol. 12, No. 7 / 1 July 2021 / Biomedical Optics Express 3934
Biomedical Optics EXPRESS

Evaluation of the changes in human milk lipid composition and conformational state with Raman spectroscopy during a breastfeed

JOHANNA R. DE WOLF,[1,*] ANKI LENFERINK,[1] AUFRIED LENFERINK,[2] CEES OTTO,[2] AND NIENKE BOSSCHAART[1]

[1]Biomedical Photonic Imaging Group, Faculty of Science and Technology, Technical Medical Centre, University of Twente, P.O. Box 217, 7500 AE Enschede, The Netherlands
[2]Medical Cell BioPhysics Group, Faculty of Science and Technology, Technical Medical Centre, University of Twente, P.O. Box 217, 7500 AE Enschede, The Netherlands
[*]j.r.dewolf@utwente.nl

Abstract: Human milk fat forms the main energy source for breastfed infants, and is highly variable in terms of concentration and composition. Understanding the changes in human milk lipid composition and conformational state during a breastfeed can provide insight into lipid synthesis and secretion in the mammary gland. Therefore, the aim of this study was to evaluate human milk fatty acid length, degree of unsaturation (lipid composition) and lipid phase (lipid conformational state) at different stages during a single breastfeed (fore-, bulk- and hindmilk). A total of 48 samples from 16 lactating subjects were investigated with confocal Raman spectroscopy. We did not observe any significant changes in lipid composition between fore-, bulk and hindmilk. A new finding from this study is that lipid conformational state at room temperature changed significantly during a breastfeed, from almost crystalline to almost liquid. This observation suggests that lipid synthesis in the mammary gland changes during a single breastfeed.

1. Introduction

Human milk is a complex mixture of macronutrients (fat, proteins, carbohydrates), micronutrients (vitamins, minerals) and bioactive factors (cells, hormones, immunoglobins and more) [1,2]. The composition of human milk is dynamic and is influenced by several factors such as stage of lactation, nursing frequency, time during the day, and maternal diet [1,3–5]. Understanding human milk composition and the origin of its large biological variation is important for optimal management of infant feeding [1], for understanding its relation to maternal diet [3,6–8], and for the improvement of formula milk composition [5,9]. Nevertheless, the origin, synthesis and secretion processes of many human milk components are not yet completely understood [7,10,11]. This also includes the lipids in human milk.

Lipids in human milk comprise 30 to 55% of its total energy content [6,8] and thereby form the main source of energy for the infant [12]. Lipids are also the most variable milk component, with concentrations changing between mothers, over the course of lactation and during single breastfeeds [1,3,4,6,9]. The fat concentration of hindmilk, defined as the last milk secreted during a feed, is two to three times higher than the fat concentration of foremilk, defined as the initial milk of a breastfeed [1,13,14]. Lipids in milk are gathered in milk fat globules [8,12]. The core of these globules consist of triacylglycerol (TAG) molecules [3,15,16] and the core is enveloped by a membrane [8,16]. TAG molecules are esters of glycerol with three fatty acids [5,8,16] as shown in Fig. 1 and these molecules make up 95 to 98% of the total lipids in human milk.

Similar to the fat concentration, the lipid composition is highly variable and is known to be strongly related to maternal diet [6,14,17]. A number of studies [3,6] examined the

#427646 https://doi.org/10.1364/BOE.427646
Journal © 2021 Received 15 Apr 2021; revised 17 May 2021; accepted 17 May 2021; published 8 Jun 2021

Biomedical Optics EXPRESS

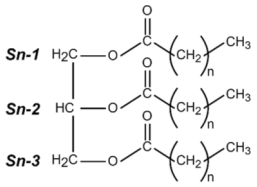

Fig. 1. The molecular structure of triacyl glycerol with the three positions (sn-1, sn-2 and sn-3) on the glycerol backbone.

lipid composition (fatty acid length and degree of unsaturation) during breastfeeds using gas chromatography. Whereas Daly et al. [3] did not find any significant differences in fatty acid saturation, Cunha et al. [6] showed that the lipid composition of fore- and hindmilk differs. They observed a significant increase in the saturated fatty acids and a decrease in the monounsaturated fatty acids during a breastfeed [6]. Besides the fatty acid composition, the distribution of the fatty acids to the glycerol backbone is not random [5] and affects the lipid phase, nutritional function, and the digestion of the lipids in the infant intestines [18]. However, it is currently unknown how the lipid phase and stereospecificity change during a single breastfeed. More knowledge about the change in lipid composition and conformational state during a breastfeed can contribute to more in-depth knowledge on the metabolic and nutritional value of lipids in human milk. In addition, this knowledge can also contribute to a better understanding of the synthesis of lipids in the mammary gland. Therefore, the aim of this study is to evaluate the change in lipid composition and conformational state of human milk during a breastfeed.

Research into the composition of human milk commonly requires costly and time-consuming chemical analysis methods such as gas chromatography, nuclear magnetic resonance and enzyme linked immunosorbent essay [2]. Optical methods for human milk composition analysis potentially offer a rapid, simple and non-destructive alternative to these chemical methods [13,19,20]. From the available optical methods, Raman spectroscopy can perform the most detailed analysis of human milk composition [15,21], but at present its application for human milk research has remained limited [2,12,15,21,22]. Previous studies with Raman spectroscopy on human milk have focused on the dependency of lipid composition on fat globules size [15], on the differences in milk composition between female and male infants [2], and on the quantification of macronutrients [21,22]. Compared to water and other milk components, the contribution of lipids to the Raman spectrum of human milk is relatively large. Many lipids have distinct Raman features, which facilitates a detailed analysis of lipid composition, such as the fatty acid length and degree of unsaturation [23]. In addition to lipid composition, Raman spectroscopy uniquely allows to investigate the conformational state of lipids [24]. Therefore, this study employed Raman spectroscopy to investigate lipid composition and conformational state in human milk during different stages of a single breastfeed.

2. Materials and methods

2.1. Human milk samples

For this research, 16 healthy volunteers between 26 and 35 years donated milk samples between April and August 2018. All volunteers lived in the Netherlands and had a lactation stage between 2 and 9 months. Only lactating subjects who gave birth to healthy, full-term infants were included. The study was approved by the Committee on Research Involving Human Subjects (dossier# 2018-487, CMO Arnhem-Nijmegen, The Netherlands), and all participants gave written consent prior to the study.

The volunteers donated extracted milk using their own breast pump. All volunteers performed single-sided milk expression, except for participant 2, who performed double-sided milk

Biomedical Optics EXPRESS

expression on both breasts. All volunteers donated three milk samples from the breast which had not been emptied for the longest period of time following a step-wise protocol. The three donated samples were (1) the first 2 to 5 mL of a breastfeed, named foremilk, (2) the last 2 to 5 mL of a breastfeed, named hindmilk and (3) 2 mL of milk from the total expressed milk volume during the same breastfeed, named bulk milk. The donated samples were cooled (between the 0 and 7 °C) for a maximum of 24 hours. After cooled transport, each sample was stored at −18 °C. Measurements were made within 3.5 months after first storage.

2.2. Sample preparation

Each sample was prepared for Raman measurements in four steps: 1) the samples were thawed in a water bath at 20–25 °C for at least one hour, 2) the samples were homogenized by inverting them approximately 5 times and by pipetting a part of the sample volume up and down until the sample was visually homogeneous, 3) Each milk sample was diluted 4 times with Phosphate Buffered Saline (PBS), 4) 50 µL of the homogenized diluted milk sample was pipetted into a microscope well glass slide (Cat. no.: 12290, BMS Microscopes) and covered with a borosilicate glass cover slip (Cat. no.: 631–0158, VWR Ltd) with a diameter of 22 mm diameter and a thickness of 0.13 mm. The cover slip was placed for $^2/_3$ over the well before the milk was pipetted into the well in order to avoid air bubbles. No sealing was applied. The samples on the microscope glass slide were placed on the object table of the confocal Raman microscope.

2.3. Confocal Raman microscopy

Raman spectra were measured with the confocal Raman microscope set-up as schematically shown in Fig. 2. The Raman microscope set-up is discussed more elaborately in Pully et al. [25]. In brief, the excitation laser of this microscope was a krypton ion laser (Innova 90-K, Coherent Inc.) with a wavelength of 647.1 nm. The dichroic beam splitter (DiO2-647RU-25, Semrock Inc.) reflected the incident light onto the scanning mirror system (General Scanning Inc.). This system was capable of shifting the focus in the x-y plane of the sample over an area of 56×56 µm with a position resolution of ~100 nm. A 40x / 0.95 NA objective (UPLSAPO, Olympus Corp.) was used to focus the incident light in the sample. The power of the incident light at the sample was 35 mW. The Raman scattered light was collected by the same objective and passed through the dichroic beam splitter and a long pass filter (Razor Edge 647, Semrock Inc.) to reduce the contribution of elastically scattered light to the signal. The Raman scattered light was detected by a 1600×200 pixel CCD camera (Newton DU970N-BV, Andor Technology) after dispersion in a home build spectrograph. A lens (Thorlabs, AC254-030-B) with a focal length of 30 mm focused the scattered light on a confocal pinhole with a diameter of 15 µm in front of the spectrograph. The spectral range from $-35\,\mathrm{cm}^{-1}$ to $3670\,\mathrm{cm}^{-1}$ was recorded with an average spectral resolution of $\sim 2.3\,\mathrm{cm}^{-1}$ per pixel. The theoretical axial and lateral resolution at the sample based on full width half maximum was 1480 nm and 365 nm, respectively.

Per sample, a total of 8100 Raman spectra was collected in a 3D volume of $88 * 10^3$ µm^3, by laying a 30×30 raster pattern over an area of 56×56 µm per layer in a total of 9 layers in depth. The measurements were started at the deepest layer in the milk (32 µm below the cover slip) and each successive layer was 4 µm above the previous layer. The top layer was closest to the cover slip, where no Raman scattered light from the cover slip could be detected. Trapping milk fat globules in the laser focus was prevented by scanning in anti-trapping mode: this mode involves non-sequential scanning in the raster pattern of each layer, with a fast motion of the focus over a large distance (≥28 µm) between successive measurement points. All Raman spectra were measured with an integration time of 200 ms in a climatised laboratory at a temperature of 20 °C.

Biomedical Optics EXPRESS

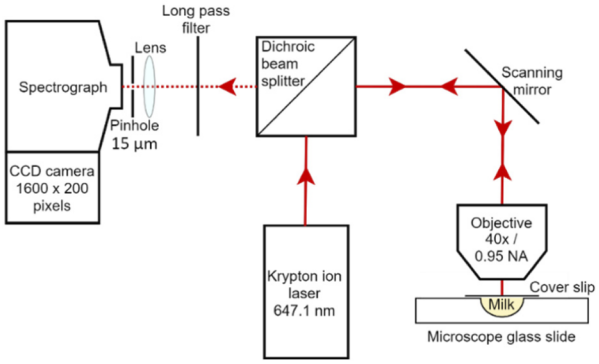

Fig. 2. A schematic drawing of the confocal Raman spectroscope. The laser light (wavelength of 647.1 nm) is reflected by the dichroic beam splitter and focussed by a 40x/0.95 NA objective on the sample. The Raman back scattered light is collected by the same objective and passes through the beam splitter and the long pass filter. The Raman spectrum is dispersed in the spectrograph and detected by the CCD camera.

2.4. Raman data processing

Pre-processing of the raw spectra consisted of four steps as displayed in Fig. 3. First, "cosmic rays", which showed up as intense spikes covering one or a few pixels, were removed from the spectra before data analysis. Next, the spectral transmission for the entire set up was corrected, which includes the wavelength sensitivity of the camera, using a tungsten halogen white light source (AvaLight-HAL, Avantes BV) with a known emission spectrum. Third, the measured spectrum was corrected for all light contributions reaching the spectrograph when there was no sample present (background). Finally, the wavelength axis was calibrated by measuring spectra from an ArHg lamp and Raman spectra of a toluene sample.

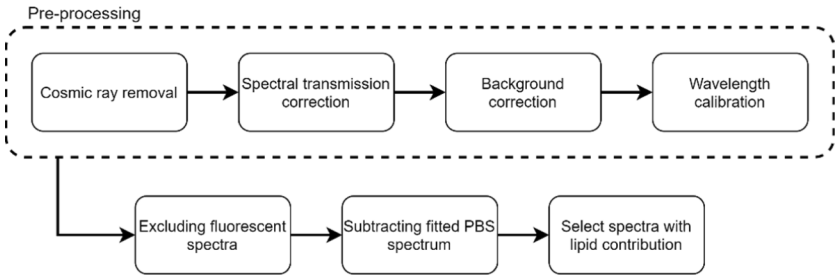

Fig. 3. Flow chart of all data processing steps executed prior to the data analysis.

After pre-processing of each raw spectrum, the spectra containing an auto-fluorescent contribution were excluded from the dataset. These spectra with an auto-fluorescent contribution possessed an elevated baseline, which reduced the signal to noise ratio of the Raman spectra. Spectra with a dominant auto-fluorescent contribution were identified using an outlier method based on Hotelling's T^2 test of the results of a principal component analysis per sample per layer. All outlier spectra were removed from the data set.

The next data processing step was to correct all spectra for the water contribution. Water present in the whey and in the solvent PBS was detectable in most of the Raman spectra. The vibrational bands from water partially overlap with the bands from lipids. Therefore, a pure PBS spectrum was measured and fitted to each individual spectrum, using a least squares algorithm. Subtraction

Biomedical Optics EXPRESS

of the fitted PBS spectrum from each individual spectrum resulted in a water-corrected Raman spectrum.

Since the focus of this study was to evaluate the lipid composition and conformational state of human milk, the last data processing step was the selection of spectra containing a significant lipid contribution. The Raman spectra predominantly measured in whey did not provide information on the lipid composition. Therefore, only spectra with a clearly observable lipid signal with respect to the noise floor (signal to noise ratio SNR $\geq$ 11) were used for data analysis. For SNR calculation, noise was defined as the maximum, I_{max}, minus the minimum, I_{min}, value in the region 1800 until 1900cm^{-1}, which is void of any human milk Raman bands. The signal was defined as the maximum intensity of the band located at 1745cm^{-1}, I_{1745}, which is related to the ester bond of the lipids. This selection resulted in an average of 4700 spectra per sample that was used for further data analysis.

$$SNR = \frac{I_{1745}}{I_{max} - I_{min}}$$

2.5. Band intensity ratio analysis

Band intensity ratios were used to quantify the lipid composition and conformational state in human milk. Each band intensity was calculated by taking the average intensity of the band and subtracting the average baseline close to the band [26]. Each average baseline had a minimum spectral width of 21 cm^{-1}. As described next, the assignment of vibrational bands was based on pure lipid spectra and literature.

3. Results

3.1. Assignment vibrational bands

The vibrational bands present in human milk Raman spectra were assigned by a combination of information from other studies [12,15,23,24,27,29] and our own measurements on pure lipid samples. The Raman spectra of these pure lipids can be found in the Supplement. The bands beyond 1060 cm^{-1} observed in human milk Raman spectra and their assignment are listed in Table 1. Bands before 1060 cm^{-1} were observed in the Raman spectra, but are not listed in Table 1 as these bands were not relevant for the analysis of the lipid composition and conformational state. The high intensity bands listed in Table 1 originated from lipids and carotenoids, due to their high Raman activity compared to other human milk components [15,23].

3.2. Raman spectra

The average Raman spectra of all fore-, bulk- and hindmilk samples over all participants are presented in Fig. 4. The bands from Table 1 are labelled. This demonstrates the large contribution of lipids and carotenes to the spectra.

Figure 4 also shows the presence of unsaturated fatty acids in the samples by three bands in the Raman spectra, namely C = C-H scissoring δ(1260), C = C stretching ν(1655) and C = C-H stretching ν(3010) as listed in Table 1. These bands have a high intensity with respect to the C-C-H twisting bands ρ(1300), C-C scissoring δ(1440) and C-H stretching ν(2850). The band δ(1260) appears as a shoulder on the ρ(1300) band in case of a low degree of unsaturated fatty acids. Furthermore, the location of two of these bands, namely ν(1655) and ν(3010), also indicates the configuration of the C = C bond [30,31].

Figure 4 also demonstrates characteristics of the lipid phase (crystalline/liquid state), in other words the mobility of the hydrocarbon chains. Lipids in the crystalline state can be recognized by the high intensity of the bands C-C stretching ν(1060), C-C stretching ν(1130) and C-H stretching antisymmetric ν(2890) with respect to the bands C-C stretching ν(1100) and C-H symmetric stretching ν(2850). Lipids in the liquid state can be recognized by a high intensity of the band

Biomedical Optics EXPRESS

Table 1. Overview of the high intensity bands observed in human milk Raman spectra

Wavenumber [cm^{-1}]	Assignment vibrational mode	Marker bands	Source
1060	C-C stretching of lipids (trans conformation)	Crystalline state lipids	Own measurements and [24,27]
1100	C-C stretching of lipids (gauche conformation)	Fluid state lipids	Own measurements and [24,27]
1130	C-C stretching of lipids (trans conformation)	Crystalline state lipids	Own measurements and [24,27]
1160	C-C stretching of carotenoids	Carotene	[12,23]
1260	C = C-H scissoring of lipids	Unsaturated lipids	[23,27]
1300	C-C-H twisting of lipids		[12,15,23,27,28]
1440	C-C bending of lipids		[27,28]
1525	C = C stretching of carotenoids	Carotene	[12,23]
1655	C = C stretching of lipids	Unsaturated lipids	[12,23,27]
1745	C = O stretching of lipids	Glyceryl backbone	Own measurements and [12,15,23,27]
2850	C-H symmetric stretching of lipids (CH2 groups of fatty acid chain)		[12,23,24,29]
2890	C-H antisymmetric stretching of lipids (CH2 groups of fatty acid chain)	Crystalline state lipids	[12,15,23,24,27,29]
2930	C-H symmetric stretching of lipids (CH3 groups of fatty acid chain)		[23,27]
3010	C = C-H stretching of lipids	Unsaturated lipids	[23,27]

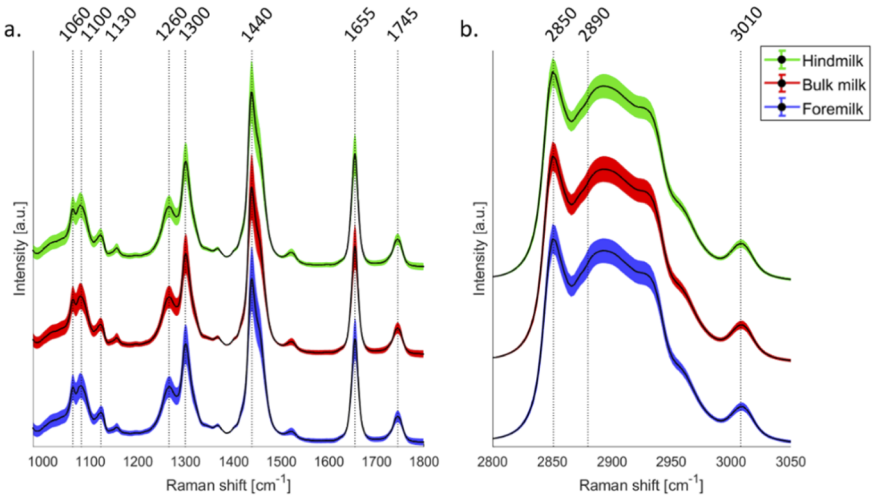

Fig. 4. The average human milk Raman spectra of all foremilk (blue), bulk milk (red) and hindmilk (green) samples for (a) the fingerprint region and (b) the high Raman shift region. The shaded regions in the spectra display the standard deviation between spectra and the solid line is the average.

Biomedical Optics EXPRESS

ν(1100). The bands ν(1060) and ν(1130) appear as a shoulder on the band ν(1100) and the band ν(2890) is no longer distinguishable from the other bands in the this spectral region.

3.3. Band intensity ratios

Three main characteristics of human milk lipid composition and conformational state were investigated with Raman spectroscopy: fatty acid length, the degree of unsaturation of the fatty acids and the lipid phase, i.e. the ratio trans and gauche conformation and the magnitude of intrachain disordering. These three characteristics were investigated using the band intensity ratios listed in Table 2.

Table 2. Overview of the band intensity ratios used with the corresponding indication

Ratio	Quantify	Source
δ(1440) / ν(1745)	Length	This work
δ(1260) / ρ(1300)	Degree of unsaturation	[12,23,31]
ν(1655) / δ(1440)	Degree of unsaturation	[12,23,27,31]
ν(1100) / ν(1130)	Rate trans and gauche conformation	[12,23,24]
ν(2850) / ν(2890)	Interchain interactions	[12,23,24]

The fatty acid length was investigated by the ratio δ(1440) / ν(1745). The intensity of the band δ(1440) is representative for the number of C-C bonds in the fatty acids [27]. The band ν(1745) originates from the ester bond and each fatty acid attached to the glycerol backbone has one ester bond, as shown in Fig. 1. Therefore, the band ν(1745) is representative for the total number of fatty acids. Thus, the intensity ratio δ(1440) / ν(1745) is representative for the length of the fatty acids present in human milk.

The degree of unsaturation was investigated by the ratios δ(1260) / ρ(1300) and ν(1655) / δ(1440)., which are also commonly used band intensity ratios in literature to assess unsaturation [12,23,27,31]. The marker bands for the presence of unsaturated fatty acids are δ(1260), ν(1655) and ν(3010) and those for saturated fatty acids are ρ(1300) and δ(1440).

The lipid phase was investigated using the two band intensity ratios ν(1100) / ν(1130) and ν(2850) / ν(2890). The band ratio ν(1100) / ν(1130) is related to the ratio tans and gauche conformations. The bands ν(1060) and ν(1130) are associated with trans conformation: the out-of-phase conformational state of the C-C bonds of the fatty acids. The band ν(1100) was associated with gauche conformation: the in-phase conformational state of the C-C bonds of the fatty acids [12,23,28]. The fatty acids in the crystalline state or solid phase contain trans conformations [28], which can be observed in the Raman spectra by the two sharp lines located at 1060 and 1130 cm^{-1} [24]. When the lipid phase shifts from crystalline to liquid, the ratio gauche to trans conformation increases. A higher number of gauche conformation results in a higher intensity of the band ν(1100), while the bands ν(1060) and ν(1130) appear as shoulder bands [23,24,28,29]. The intensity ratio ν(2850) / ν(2890) is sensitive to the interchain packing and intrachain conformational disorder of lipids [24,28,29]. The lipids in the liquid phase have a higher magnitude of disordering and this is related to a decrease in the band intensity of ν(2890) [24,28].

3.3.1. Fatty acid length

The fatty acid length was quantified using the band intensity ratio δ(1440) / ν(1745) as listed in Table 2. A high value of this intensity ratio indicates a larger contribution of long fatty acids. The median values of this intensity ratio are shown in Fig. 5. Figure 5(a) demonstrates that the median fatty acid length was different for samples donated by different participants. No significant difference in the fatty acid length can be observed between fore-, bulk- and hindmilk

Biomedical Optics EXPRESS

samples of individual participants. Figure 5(b) shows the median intensity ratio of samples donated by all participants. This also confirms that no significant difference was present between the fatty acid lengths of fore-, bulk-, and hindmilk.

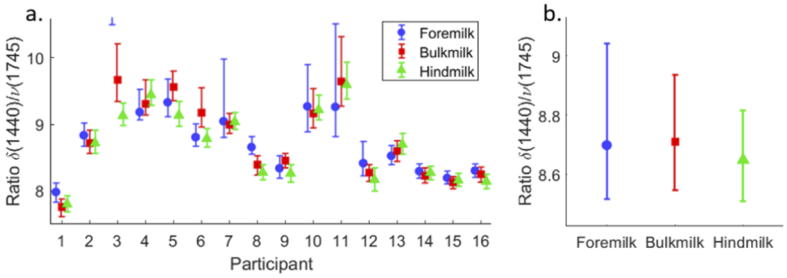

Fig. 5. Band intensity ratio δ(1440)/ν(1745) for (a) foremilk, bulk milk, and hindmilk samples for each participant and (b) median ratio values for each milk type over all 16 participants. Data points represent median values, error bars represent 25th and 75th percentiles. A high value of the ratio δ(1440)/ν(1745) indicates a larger contribution of long fatty acids.

The band intensity ratio δ(1440) / ν(1745) was also used to quantify the average fatty acid length per spectrum. Raman spectroscopic measurements on the pure saturated lipids glyceryl trimyristate (14:0, TMA), glyceryl tripalmitate (16:0, TPA) and glyceryl tristearate (18:0, TSA) indicated that the band intensity ratio δ(1440) / ν(1745) increased linearly with the fatty acid length. Using this information, we determined that the median value of the fatty acid length in human milk was 17.19 ± 0.18 carbon atoms. The milk samples with the shortest and longest fatty acids had a median value of 16.02 ± 0.20 and 18.39 ± 0.29 carbon atoms per fatty acid, respectively.

The exceptionally high value for the ratio δ(1440) / ν(1745) of 11.82 of the foremilk sample of participant 3 was considered as an outlier (not shown in Fig. 5(a)). This is potentially the result of a low fat concentration in combination with a high lactose concentration, as both components contribute to the intensity of the band at $1745 cm^{-1}$.

3.3.2. Degree of unsaturation of fatty acids

The band intensity ratios δ(1260) / ρ(1300) and ν(1655) / δ(1440) were used to investigate the degree of unsaturation of the fatty acids in human milk. A high value of these ratios reveal a high degree of unsaturation. Figure 6 presents the median values for these two ratios for the different samples. Figures 6(a) and 6(c) demonstrate differences in the degree of unsaturation of the fatty acids between samples donated by different participants. Figures 6(b) and 6(d) indicate no significant difference in the degree of unsaturation of fatty acids from fore-, bulk- and hindmilk.

The band intensity ratios were also used to quantify the median number of double bonds per 16 single bonds of the fatty acids present in human milk. It was assumed that the intensity of the bands δ(1260) and ν(1655) linearly increases with the number of double bonds of the fatty acids, as has been shown by Weng et al. [31] and Czamara et al. [27]. Raman spectroscopic measurements on the pure lipids TSA, glyceryl trioleate (18:1, TOA) and glyceryl trilinoleate (18:2, TLA) were used to calculate the median value of double bonds per 16 single bonds for the fatty acids present in human milk. Using this information, the median value of double bonds per 16 single bonds in the fatty acids of human milk was 0.922 ± 0.023. The milk samples with the highest and lowest degree of unsaturation had 0.979 ± 0.011 and 0.85 ± 0.03 double bonds per 16 single bonds, respectively.

Biomedical Optics EXPRESS

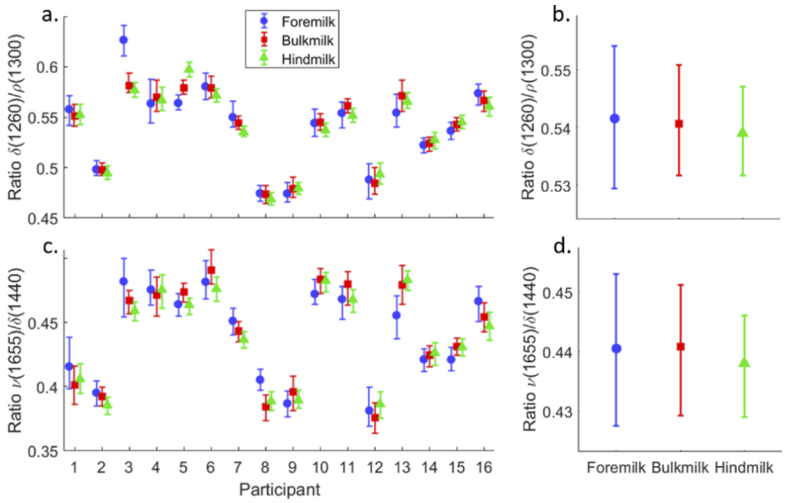

Fig. 6. Band intensity ratios for (a, c) foremilk, bulk milk and hindmilk samples for each participant and (b, d) median ratio values for each milk type over all 16 participants for the ratios δ(1260) / ρ(1300) and ν(1655) / δ(1440), respectively. Data points represent median values, error bars represent 25th and 75th percentiles. A high value of the ratios δ(1260) / ρ(1300) and ν(1655) / δ(1440) indicates a higher degree of unsaturation of the fatty acids.

3.3.3. Lipid phase

The band intensity ratios ν(1100) / ν(1130) and ν(2850) / ν(2890) were used to investigate the lipid phase of human milk. Figure 7 presents the ratios, indicating the mobility of the lipid bonds of the samples. A trend of increasing lipid bond mobility from foremilk to hindmilk can be observed for each participant (Figs. 7(a) and 7(c)), as well as for the median ratios over all

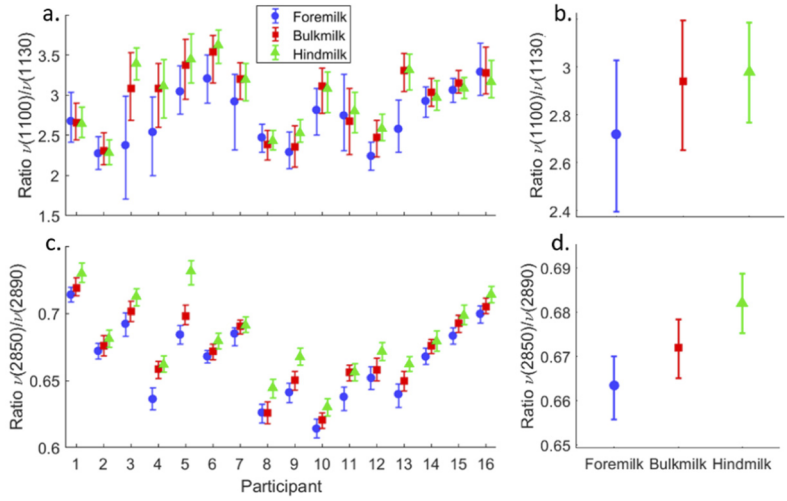

Fig. 7. Band intensity ratios for (a, c) foremilk, bulk milk and hindmilk samples for each participant and (b, d) median ratio values for each milk type over all 16 participants for the ratios ν(1100) / ν(1130) and ν(2850) / ν(2890), respectively. Data points represent median values, error bars represent 25 and 75 percentiles. A high value of the ratios ν(1100) / ν(1130) and ν(2850) / ν(2890) indicates that the fatty acids are more in liquid state.

Biomedical Optics EXPRESS

participants (Figs. 7(b) and 7(d)). The ratio ν(1100) / ν(1130) presented in Figs. 7(a) and 7(b) indicates a higher presence of gauche conformation in the lipid chains of hindmilk samples than foremilk samples, corresponding to a more fluid state of the hindmilk lipids at room temperature. The ratio ν(2850) / ν(2890) presented in Figs. 7(c) and 7(d) indicates a significant difference with 2.8% in magnitude of disordering of the lipid chains between foremilk and hindmilk. Thus, the lipids in foremilk were in a more crystalline state and the lipids in hindmilk were in a more fluid state for our human milk measurements at room temperature. In addition, Figs. 7(a) and 7(c) demonstrate high variability between participants in the phase of the lipids.

To illustrate the difference in lipid phase between Raman spectra of human milk, Figs. 8(a) and 8(b) show two examples of individual, unaveraged Raman spectra: one spectrum with a high degree of lipids in the crystalline phase (foremilk sample participant 4) and one spectrum with a high degree of lipids in the liquid phase (hindmilk sample participant 4). The sharp lines of the bands ν(1060) and ν(1130) can be clearly observed in the crystalline phase spectrum from the foremilk sample, indicating that the fatty acids contain more trans, than gauche conformations. The higher intensity of these bands is also confirmed by the Raman difference spectrum in Figs. 8(c) and 8(d). Furthermore, the band ν(2890) cannot be clearly distinguished from the other bands in the high Raman shift region of the liquid phase spectrum from the hindmilk sample, while this band can be observed in the crystalline phase spectrum. The Raman difference spectrum in Figs. 8(c) and 8(d) also confirms the higher intensity around 2890 cm^{-1} for the crystalline phase spectrum. The Raman difference spectrum in Figs. 8(c) and 8(d) also reveals two other differences in case of crystalline lipids compared to liquid lipids. First, a shift of the band ρ(1300) from 1302 to 1297 cm^{-1}. Second, a better distinguishable shoulder band on

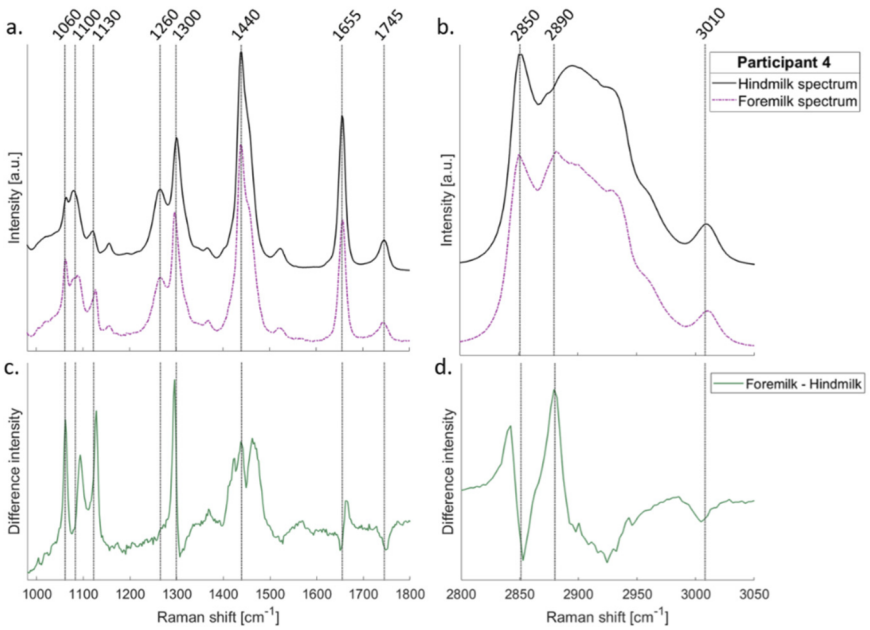

Fig. 8. Two typical, individual Raman spectra of fore- and hindmilk samples donated by participant 4 in a) the fingerprint region and b) the high Raman shift region. (c, d) show the difference between the two spectra in both regions. The foremilk spectrum shows features of lipids in a more crystalline state and the hindmilk spectrum shows features of lipids in a more liquid state. The Raman difference spectrum demonstrates the intensity differences between the crystalline- and liquid phase lipid spectra.

Biomedical Optics EXPRESS

the δ(1440) band located at 1460 cm^{-1}. All these differences together demonstrate that the magnitude of disordering of the lipids was different for these two spectra.

4. Discussion

In this study, the difference between fore-, bulk- and hindmilk in the lipid composition and conformational state of human milk was investigated using Raman spectroscopy. Knowledge about lipid composition and conformational state is relevant for understanding the origin, synthesis and secretion of the lipids in human milk. To assess lipid composition, both the median length and the median degree of unsaturation of the fatty acids per sample were quantified. To assess lipid conformational state, the number of trans and gauche conformations and the magnitude of intrachain disordering was investigated.

As 95% to 98% of the lipids in human milk are TAG molecules in the core of milk fat globules [3,5,8,11,21], the vibrational bands observed in Raman spectra of human milk mainly originate from these TAG molecules. Thus, our findings on lipid composition and conformational state can be ascribed predominantly to TAG molecules.

4.1. Fatty acid length

In this study, we measured a median fatty acid length of 17.19 carbon atoms per fatty acid. This is in agreement with literature, where the fatty acid length was measured by gas chromatography [6,14]. Cunha et al. [6] reported an average length of 17.06 carbon atoms per fatty acid for human milk samples donated by Brazilian women and Yuhas et al. [14] reported an average length per fatty acid of 16.91 carbon atoms for human milk donated by women from the US. Additionally, we concluded that the median fatty acid length was not significantly different between foremilk, bulk milk and hindmilk. These results are also consistent with the results reported by Daly et al. [3], Saarela et al. [4] and Cunha et al. [6]. Furthermore, our study revealed differences in the median fatty acid length between samples donated by different participants. Also this finding is in agreement with other studies on the lipid composition of human milk samples [5,14].

4.2. Degree of unsaturation of fatty acids

The results of this study did not reveal a significant difference between the degree of unsaturation of fatty acids of fore-, bulk- and hindmilk samples. This is in agreement with the results from Daly et al. [3]. However, Cunha et al. [6] showed a significant increase in the saturated fatty acids and a decrease in the monounsaturated fatty acids of human milk during a breastfeed. The change in the lipid composition reported by Cunha et al. [6] was small, with an increase in saturated fatty acids from 40.7% in foremilk to 42.33% in hindmilk and a decrease in monounsaturated fatty acids from 34.5% in foremilk to 32.13% in hindmilk. Furthermore, Cunha et al. [6] reported a non-significant increase in the polyunsaturated fatty acids during a breastfeed. Whereas the results of Cunha et al. [6] were based on gas chromatography, the measurements in this study were performed with a confocal Raman spectroscope. As the Raman scattered light from all molecules in the focus was collected simultaneously, our methodology is insensitive to single fatty acids and cannot differentiate between the saturated, monounsaturated and polyunsaturated fatty acids. This difference in methodology, combined with the small changes in the degree of unsaturation presented by Cunha et al. [6] explains why this study did not demonstrate a change in the degree of unsaturation of the fatty acids in foremilk and hindmilk.

The location of the C = C stretching band and the C = C-H stretching band display the configuration of the C = C bond [15,30,31]. The centres of these vibrational bands in the human milk Raman spectra of this study were located at 1655 and 3010 cm^{-1}, respectively. This corresponds to C = C bonds in the cis configuration. No bands were observed at the locations 1670 and 3000 cm^{-1}, which corresponds to C = C bonds in the trans conformation. Thus, the

Biomedical Optics EXPRESS

configuration of the majority of the C = C bonds of unsaturated fatty acids in human milk were in the cis configuration.

In this study, the median value of degree of unsaturation of the fatty acids in human milk (0.92 C = C per 16 C-C) was slightly higher than reported by other studies using gas chromatography. Cunha et al. [6] reported an average degree of unsaturation of human milk of Brazilian women of approximately 0.88 C = C per 16 C-C and Yuhas et al. [14] reported an average degree of unsaturation for women from the United states of 0.80 C = C per 16 C-Cs. It should be noted that the lipid composition of human milk was also influenced by maternal diet [6,16], which can explain the slightly higher degree of unsaturation of fatty acids measured in this study, as well as the large variability between participants.

4.3. Lipid phase

The most striking result from this study is the difference in lipid phase between human fore-, bulk- and hindmilk samples at room temperature. We measured an increase of 2.8% in lipid phase during a breastfeed from a more crystalline, to a more liquid state. Milk fat at room temperature is in a mixed crystalline/liquid state [23]. Whereas lipid phase is influenced by both its molecular structure and temperature, all measurements were performed under the same circumstances at an actively controlled room temperature of 20 °C. As there is virtually no absorption at the laser wavelength of 647 nm, the temperature of the sample in the laser focus has been assumed to be identical to room temperature. The lipid phase at room temperature is therefore expected to be influenced only by the degree of unsaturation of the fatty acids, the length of the fatty acids and the stereospecific position of the fatty acids on the glycerol backbone [23,24,28,29]. As our results indicate that there is no change in the length or degree of unsaturation of the fatty acids (Figs. 5 and 6), we argue that the change in lipid phase during a breastfeed is predominantly caused by a change in the stereospecific position of the fatty acids to the glycerol backbone during a breastfeed. We therefore hypothesize that the esterification process of TAG molecules changes during a breastfeed.

The esterification of TAG molecules determines the stereospecific position of fatty acids, where the distribution of the fatty acids to the glycerol backbone is not random [5]. Several studies have shown that the stereospecific position of fatty acids greatly influences the lipid digestion and absorption [18,32]. In human milk, palmitic acid (PA) (16:0) is predominantly esterified at the sn-2 position (40–70%) [5,18,32,33] and oleic acid (18:0) is predominantly esterified at the sn-1 position [33,34]. Barbano et al. [35] showed that TAGs at room temperature were mostly in fluid state when the fatty acid palmitic acid was esterified on the sn-1 position and milk TAGs were mostly in the crystalline state when palmitic acid was esterified on the sn-2 position [35]. Further research is necessary on the exact causes of the change in human milk lipid phase at room temperature. This may provide more insight into the potential relation between lipid phase, the stereospecific position of the fatty acids, and the nutritional properties and digestion of the lipids in human milk.

5. Conclusion

The aim of this study was to examine the differences in lipid composition and conformational state between human fore-, bulk- and hindmilk with Raman spectroscopy. Our results are in agreement with existing literature on this topic, i.e., no difference in the length or degree of unsaturation could be observed between fore-, bulk- and hindmilk. A new finding of this study is that the lipid phase in human fore-, bulk- and hindmilk is significantly different at room temperature, with lipids from foremilk in a more crystalline state and lipids from hindmilk in a more fluid state. This study raises important questions about the origin, synthesis and function of the milk fat globules in human milk. Further research is required to understand the biological function of the change in the lipid phase during a breastfeed.

Biomedical Optics EXPRESS

Funding. Pioneers in Health Care Innovation Fund, University of Twente.

Acknowledgments. We thank Dayna Every for her contribution to the initial data analysis and we gratefully acknowledge all lactating subjects for donating milk samples.

Disclosures. The authors declare that there are no conflicts of interest related to this article.

Data availability. Data underlying the results presented in this paper are not publicly available at this time but may be obtained from the authors upon reasonable request.

Supplemental document. See Supplement 1 for supporting content.

References

1. O. Ballard and A. L. Morrow, "Human milk composition: nutrients and bioactive factors," Pediatr. Clin. North Am. **60**(1), 49–74 (2013).
2. R. Ullah, S. Khan, S. Javaid, H. Ali, M. Bilal, and M. Saleem, "Raman spectroscopy combined with a support vector machine for differentiating between feeding male and female infants mother's milk," Biomed. Opt. Express **9**(2), 844–851 (2018).
3. S. Daly, A. Di Rosso, R. A. Owens, and P. E. Hartmann, "Degree of breast emptying explains changes in the fat content, but not fatty acid composition, of human milk," Exp Physiol **78**(6), 741–755 (1993).
4. T. Saarela, J. Kokkonen, and M. Koivisto, "Macronutrient and energy contents of human milk fractions during the first six months of lactation," Acta Paediatrica. **94**(9), 1176–1181 (2007).
5. W. Wei, Q. Jin, and X. Wang, "Human milk fat substitutes: Past achievements and current trends," Prog. Lipid Res. **74**, 69–86 (2019).
6. J. da Cunha, T. H. M. da Costa, and M. K. Ito, "Influences of maternal dietary intake and suckling on breast milk lipid and fatty acid composition in low-income women from Brasilia, Brazil," Early Hum. Dev. **81**(3), 303–311 (2005).
7. H. Demmelmair, M. Baumheuer, B. Koletzko, K. Dokoupil, and G. Kratl, "Investigation of long-chain polyunsaturated fatty acid metabolism in lactating women by means of stable isotope techniques," in *Bioactive Components of Human Milk*, (Academic, 2001), pp. 169–177.
8. C. Lopez, "Milk fat globules enveloped by their biological membrane: Unique colloidal assemblies with a specific composition and structure," Curr. Opin. Colloid Interface Sci. **16**(5), 391–404 (2011).
9. L. R. Mitoulas, J. C. Kent, D. B. Cox, R. A. Owens, J. L. Sherriff, and P. E. Hartmann, "Variation in fat, lactose and protein in human milk over 24 h and throughout the first year of lactation," British Journal of Nutrition. **88**(1), 29–37 (2002).
10. M. Grunewald, C. Hellmuth, F. F. Kirchberg, M. L. Mearin, R. Auricchio, G. Castillejo, I. R. Korponay-Szabo, I. Polanco, M. Roca, and S. L. Vriezinga, "Variation and interdependencies of human milk macronutrients, fatty acids, adiponectin, insulin, and IGF-II in the European PreventCD Cohort," Nutrients **11**(9), 2034 (2019).
11. H. W. Heid and T. W. Keenan, "Intracellular origin and secretion of milk fat globules," Eur. J. Cell Biol. **84**(2-3), 245–258 (2005).
12. Y. Yao, G. Zhao, Y. Yan, H. Mu, Q. Jin, X. Zou, and X. Wang, "Milk fat globules by confocal Raman microscopy: Differences in human, bovine and caprine milk," Food Res. Int. **80**, 61–69 (2016).
13. C. Veenstra, A. Lenferink, W. Petersen, W. Steenbergen, and N. Bosschaart, "Optical properties of human milk," Biomed. Opt. Express **10**(8), 4059–4074 (2019).
14. R. Yuhas, K. Pramuk, and E. L. Lien, "Human milk fatty acid composition from nine countries varies most in DHA," Lipids **41**(9), 851–858 (2006).
15. N. Argov, S. Wachsmann-Hogiu, S. L. Freeman, T. Huser, C. B. Lebrilla, and J. B. German, "Size-dependent lipid content in human milk fat globules," J. Agric. Food Chem. **56**(16), 7446–7450 (2008).
16. C. Lopez, V. Briard-Bion, O. Ménard, E. Beaucher, F. Rousseau, J. Fauquant, N. Leconte, and B. Robert, "Fat globules selected from whole milk according to their size: Different compositions and structure of the biomembrane, revealing sphingomyelin-rich domains," Food Chemistry **125**(2), 355–368 (2011).
17. L. R. Mitoulas, L. C. Gurrin, D. A. Doherty, J. L. Sherriff, and P. E. Hartmann, "Infant intake of fatty acids from human milk over the first year of lactation," Br J Nutr **90**(5), 979–986 (2003).
18. C. C. Akoh and G. Pande, "Structured Lipids and Health," Bailey's Industrial Oil and Fat Products. 1–17 (2005).
19. G. Fusch, N. Rochow, A. Choi, S. Fusch, S. Poeschl, A. O. Ubah, S.-Y. Lee, P. Raja, and C. Fusch, "Rapid measurement of macronutrients in breast milk: How reliable are infrared milk analyzers?" Clinical Nutrition **34**(3), 465–476 (2015).
20. C. Veenstra, D. Every, W. Petersen, J. B. Van Goudoever, W. Steenbergen, and N. Bosschaart, "Dependency of the optical scattering properties of human milk on casein content and common sample preparation methods," J. Biomed. Opt. **25**(04), 1 (2020).
21. K. Bērziņš, S. D. Harrison, C. Leong, S. J. Fraser-Miller, M. J. Harper, A. Diana, R. S. Gibson, L. A. Houghton, and K. C. Gordon, "Qualitative and quantitative vibrational spectroscopic analysis of macronutrients in breast milk," Spectrochim. Acta, Part A **246**, 118982 (2021).
22. M. M, E. d. Carmo, R. A. Zângaro, and L. Silveira Jr, "Quantitative determination of the human breast milk macronutrients by near-infrared Raman spectroscopy," Proc. SPIE **8229**, 82291F (2012).

Biomedical Optics EXPRESS

23. S. Gallier, K. C. Gordon, R. Jiménez-Flores, and D. W. Everett, "Composition of bovine milk fat globules by confocal Raman microscopy," Int. Dairy J. **21**(6), 402–412 (2011).
24. A. Dmitriev and N. Surovtsev, "Temperature-dependent hydrocarbon chain disorder in phosphatidylcholine bilayers studied by Raman spectroscopy," J. Phys. Chem. B **119**(51), 15613–15622 (2015).
25. V. V. Pully, A. Lenferink, and C. Otto, "Hybrid Rayleigh, Raman and two-photon excited fluorescence spectral confocal microscopy of living cells," J. Raman Spectrosc. **41**(6), 599–608 (2010).
26. A. Kunstar, C. Otto, M. Karperien, C. van Blitterswijk, and A. van Apeldoorn, "Raman microspectroscopy: a noninvasive analysis tool for monitoring of collagen-containing extracellular matrix formation in a medium-throughput culture system," Tissue Eng., Part C **17**(7), 737–744 (2011).
27. K. Czamara, K. Majzner, M. Z. Pacia, K. Kochan, A. Kaczor, and M. Baranska, "Raman spectroscopy of lipids: a review," J. Raman Spectrosc. **46**(1), 4–20 (2015).
28. C. B. Fox, R. H. Uibel, and J. M. Harris, "Detecting phase transitions in phosphatidylcholine vesicles by Raman microscopy and self-modeling curve resolution," J. Phys. Chem. B **111**(39), 11428–11436 (2007).
29. N. Surovtsev, N. Ivanisenko, K. Y. Kirillov, and S. Dzuba, "Low-temperature dynamical and structural properties of saturated and monounsaturated phospholipid bilayers revealed by Raman and spin-label EPR spectroscopy," J. Phys. Chem. B **116**(28), 8139–8144 (2012).
30. Z. Movasaghi, S. Rehman, and I. U. Rehman, "Raman spectroscopy of biological tissues," Appl. Spectrosc. Rev. **42**(5), 493–541 (2007).
31. Y.-M. Weng, R.-H. Weng, C.-Y. Tzeng, and W. Chen, "Structural analysis of triacylglycerols and edible oils by near-infrared Fourier transform Raman spectroscopy," Appl. Spectrosc. **57**(4), 413–418 (2003).
32. T. Karupaiah and K. Sundram, "Effects of stereospecific positioning of fatty acids in triacylglycerol structures in native and randomized fats: a review of their nutritional implications," Nutr. Metab. **4**(1), 16–17 (2007).
33. W. N. Ratnayake and C. Galli, "Fat and fatty acid terminology, methods of analysis and fat digestion and metabolism," Ann. Nutr. Metab. **55**(1-3), 8–43 (2009).
34. I. Haddad, M. Mozzon, and N. G. Frega, "Trends in fatty acids positional distribution in human colostrum, transitional, and mature milk," Eur. Food Res. Technol. **235**(2), 325–332 (2012).
35. D. Barbano and J. Sherbon, "Stereospecific analysis of high melting triglycerides of bovine milk fat and their biosynthetic origin," J. Dairy Sci. **58**(1), 1–8 (1975).